THEORETICAL MODEL OF TEMPERATURE MEASUREMENT

A. COUPLING BETWEEN KERR ROTATION ANGLE AND MAGNETIZATION

When an applied magnetic field ($\overrightarrow{H_{applied}}$) is excited in a direction perpendicular to the surface of an Ni nanofilm, a magnetization ($\vec{M}$) is generated within the medium due to the magnetization effect. At this point, the Ni nanofilm produces a polar MOKE， if a beam of linearly polarized light is directed at the Ni nanofilm medium. After the linearly polarized light passes through an Ni nanofilm with a fixed refractive index, the angle of polarization of the reflected light changes relative to the incident light by a value φ, as shown in Fig. 1. The linearly polarized light emitted by the laser splits into two transmission paths when it hits the interface of the Ni nanofilm medium. In one path, the linearly polarized light first enters the Ni nanofilm medium from the air, and is then reflected at interface II, modulated by the $\vec{M}$ of the film, before finally being emitted through interface I. In the other path, the linearly polarized light enters the Ni nanofilm medium from the air and is then absorbed by the silicon wafer substrate.

According to Maxwell's equations, the relationship between the magnetic field intensity vector $\vec{H}$ and the electric field intensity vector $\vec{E}$ for a linearly polarized light wave[5,6]can be expressed as:

$$\begin{cases} \nabla \times \vec{E} = -\mu_0 \dfrac{\partial \vec{H}}{\partial t} \\ \nabla \times \vec{H} = -\varepsilon_0 \boldsymbol{\varepsilon} \dfrac{\partial \vec{E}}{\partial t} \end{cases} \tag{1}$$

where ε_0 is the dielectric constant in a vacuum, μ_0 is the magnetic permeability in a vacuum, and $\boldsymbol{\varepsilon}$ is the dielectric constant tensor[4] of an Ni nanofilm, which can be expressed as:

$$\boldsymbol{\varepsilon} = \begin{vmatrix} \varepsilon_x & i\varepsilon_x Q & 0 \\ -i\varepsilon_x Q & \varepsilon_x & 0 \\ 0 & 0 & \varepsilon_z \end{vmatrix} = \begin{vmatrix} \varepsilon_x & i\varepsilon_x AM & 0 \\ -i\varepsilon_x AM & \varepsilon_x & 0 \\ 0 & 0 & \varepsilon_z \end{vmatrix} \tag{2}$$

where i is the imaginary unit, Q is the MO Voigt constant for the polar MOKE, M is the magnetization amplitude of the Ni nanofilm, ε_x and ε_z are the components of the dielectric constant tensor $\boldsymbol{\varepsilon}$ in the x and z directions, respectively, and A is the complex constant of the Ni nanofilm, which is determined from the MO Voigt constant[5,6] Q and the magnetization amplitude M measured at room temperature.

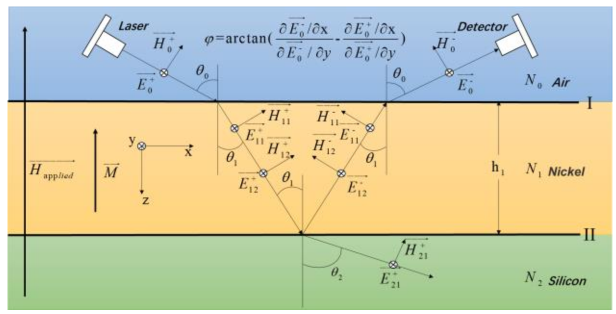

FIG. 1. Optical transfer path and electromagnetic field analysis of Ni nanofilms, where $\overrightarrow{\boldsymbol{H_{applied}}}$ is the applied magnetic field strength, $\vec{\boldsymbol{M}}$ is the magnetization in the magneto-optical layer, $\boldsymbol{N_0}$ is the refractive index of Air, $\boldsymbol{N_1}$ is the refractive index of the Ni nanofilm, $\boldsymbol{N_2}$ is the refractive index of the silicon wafer substrate, and $\boldsymbol{h_1}$ is the thickness of the Ni nanofilm. At interface **I** : incident electric field $\overrightarrow{\boldsymbol{E_0^+}}$, incident magnetic field $\overrightarrow{\boldsymbol{H_0^+}}$, reflected electric field $\overrightarrow{\boldsymbol{E_0^-}}$, reflected magnetic field $\overrightarrow{\boldsymbol{H_0^-}}$, refracted electric field $\overrightarrow{\boldsymbol{E_{11}^+}}$, refracted magnetic field $\overrightarrow{\boldsymbol{H_{11}^+}}$, incident electric field $\overrightarrow{\boldsymbol{E_{11}^-}}$,, which refers to incidence from the medium Air to interface **I**, incident magnetic field $\overrightarrow{\boldsymbol{H_{11}^-}}$, incidence from the medium Air to interface **I**. At interface **II**: incident electric field $\overrightarrow{\boldsymbol{E_{12}^+}}$, incident magnetic field $\overrightarrow{\boldsymbol{H_{12}^+}}$, reflected electric field $\overrightarrow{\boldsymbol{E_{12}^-}}$, reflected magnetic field $\overrightarrow{\boldsymbol{H_{12}^-}}$, refracted electric field $\overrightarrow{\boldsymbol{E_{21}^+}}$, refracted magnetic field $\overrightarrow{\boldsymbol{H_{21}^+}}$. $\boldsymbol{\varphi}$ denotes the phase change of $\overrightarrow{\boldsymbol{E_0^-}}$ with respect to $\overrightarrow{\boldsymbol{E_0^+}}$. $\boldsymbol{\theta_0}$ denotes the angle of incidence of light at interface **I**, $\boldsymbol{\theta_1}$ is the angle of refraction of light at interface **I**, and $\boldsymbol{\theta_2}$ is the angle of refraction of light at interface **II**. The direction of incidence is given a positive sign and the direction of reflection is given a negative sign.

The propagation of linearly polarized light along a unit vector $\vec{r} = (r_x, r_y, r_z)$ in an Ni nanofilm medium can be expressed as:

$$\begin{cases} \vec{E} = E_A \exp\left\{i\left[\omega t - \frac{2\pi N}{\lambda}(r_x x + r_y y + r_z z)\right]\right\} \\ \vec{H} = H_A \exp\left\{i\left[\omega t - \frac{2\pi N}{\lambda}(r_x x + r_y y + r_z z)\right]\right\} \end{cases} \tag{3}$$

where E_A is the amplitude of the electric field vector $\vec{E}$ of linearly polarized light, H_A is the amplitude of the magnetic field vector $\vec{H}$ of linearly polarized light, i is the imaginary unit, λ is the wavelength of a plane wave in a vacuum, ω is the angular frequency of linearly polarized light, and N is the refractive index.

Substituting Equations (2) and (3) into Equation (1), we obtain the refractive index N as:

$$N_\pm = \sqrt{\varepsilon_x \pm \varepsilon_x Q} = \sqrt{\varepsilon_x}\sqrt{1 \pm Q} \approx \sqrt{\varepsilon_x}\left(1 \pm \frac{Q}{2}\right) = \sqrt{\varepsilon_x}\left(1 \pm \frac{\mathrm{AM}}{2}\right) \quad (3)$$

From Equation (4), it can be found that for a polar MOKE, when a beam of linearly polarized light propagates along the direction of the magnetization intensity in a Ni nanofilm medium, there are two counter-rotating circularly polarized beams of light. N_+ and N_- correspond to the complex refractive indices of right and left circularly polarized light[7] φ_+ and φ_- are the phase changes after the reflection of right and left circularly polarized light, respectively. Due to the magnetization intensity, left and right circularly polarized light propagate through the medium at different speeds, and their corresponding refractive indices are different. However, due to the difference in the refractive indices, the phases of the left and right circularly polarized light finally emitted are different, yielding the Kerr deflection angle expressed as:

$$\theta_k = \frac{1}{2}|\varphi_+ - \varphi_-| \quad (5)$$

The phase change φ of the polarized light[3] after reflection through an Ni-plated film on a silicon substrate is：

$$\varphi = \arctan\frac{i\eta_0(CB^* - BC^*)}{\eta_0^2 BB^* - BC^*} \quad (6)$$

where η_0 is the conductance of air, i is the imaginary unit, $*$ is the conjugate operator, and B and C make up the characteristic matrix $\begin{bmatrix} B \\ C \end{bmatrix}$ of an Ni-plated film on a silicon substrate. The phase φ can be derived from the characteristic matrix.

The expression $\begin{bmatrix} B \\ C \end{bmatrix}$ for the characteristic matrix of an Ni-plated thin film on silicon is derived as follows.

Combining Equations (1) and (3) yields:

$$\vec{H} = Y(\vec{r} \times \vec{E}) = N\sqrt{\frac{\varepsilon_0}{\mu_0}}(\vec{r} \times \vec{E}) \quad (7)$$

Maxwell's boundary conditions indicate that the tangential components of the magnetic and electric fields are continuous on both sides of interface I. In combination with Equation (7), the relationship between the field vector in the air and the electric field vector before the change in the magneto-optical layer can be obtained as follows:

$$\begin{bmatrix} \overrightarrow{E_0} \\ \overrightarrow{H_0} \end{bmatrix} = \begin{bmatrix} 1 & 1 \\ N_1\sqrt{\frac{\varepsilon_0}{\mu_0}}\cos\theta_1 & -N_1\sqrt{\frac{\varepsilon_0}{\mu_0}}\cos\theta_1 \end{bmatrix} \begin{bmatrix} \overrightarrow{E_{11}^+} \\ \overrightarrow{E_{11}^-} \end{bmatrix} \quad (8)$$

where N_1 is the complex refractive index of the Ni nanofilm, θ_1 is the angle of refraction at interface I, the electric field vector in air $\overrightarrow{E_0}$ satisfies the expression $\overrightarrow{E_0} = \overrightarrow{E_0^+} + \overrightarrow{E_0^-} = \overrightarrow{E_{11}^+} + \overrightarrow{E_{11}^-}$, and the magnetic field vector in the air $\overrightarrow{H_0}$ satisfies the expression $\overrightarrow{\overrightarrow{H_0} = H_0^+ \cos\theta_0 - \overrightarrow{H_0^-}\cos\theta_0 = \overrightarrow{H_{11}^+}\cos\theta_1 - \overrightarrow{H_{11}^-}\cos\theta_1}$. The phase of the electric field vector in the magneto-optical layer (Ni) of the Ni-plated film on silicon can be expressed as：

$$\begin{bmatrix} \overrightarrow{E_{11}^+} \\ \overrightarrow{E_{11}^-} \end{bmatrix} = \begin{bmatrix} e^{i\delta_1} & 0 \\ 0 & e^{-i\delta_1} \end{bmatrix} \begin{bmatrix} \overrightarrow{E_{12}^+} \\ \overrightarrow{E_{12}^-} \end{bmatrix} \quad (9)$$

Where δ_1 is the phase difference between the linearly polarized light that propagates in the magneto-optical layer (Nickel) through interface I and interface II, $\delta_1 = \frac{2\pi}{\lambda}N_1 \mathrm{h}_1 \cos\theta_1$.

Maxwell's boundary conditions also indicate that the tangential components of the magnetic and electric fields are continuous on both sides of interface II. Again in combination with (7), the relationship between the changed electric field vector in the magneto-optical layer and the field vector in the substrate can be obtained as follows：

$$\begin{bmatrix} \overrightarrow{E_{12}^{+}} \\ \overrightarrow{E_{12}^{-}} \end{bmatrix} = \begin{bmatrix} \frac{1}{2} & \frac{1}{2N_1 cos\theta_1}\sqrt{\frac{\mu_0}{\varepsilon_0}} \\ \frac{1}{2} & -\frac{1}{2N_1 cos\theta_1}\sqrt{\frac{\mu_0}{\varepsilon_0}} \end{bmatrix} \begin{bmatrix} \overrightarrow{E_2} \\ \overrightarrow{H_2} \end{bmatrix} \tag{10}$$

where the electric field vector $\overrightarrow{E_2}$ in the substrate wafer satisfies the relation $\overrightarrow{E_2} = \overrightarrow{E_{12}^{+}} + \overrightarrow{E_{12}^{-}} = \overrightarrow{E_{21}^{+}}$ and the magnetic field vector $\overrightarrow{H_2}$ in the substrate wafer satisfies the relation $\overrightarrow{H_2} = \overrightarrow{H_{12}^{+}} + \overrightarrow{H_{12}^{-}} = \overrightarrow{H_{21}^{+}}$. For Ni-plated nanofilms on silicon wafers, because there is only outgoing light and no reflected light on the substrate side of interface II, the joint Equation (7) gives：

$$\overrightarrow{H_2} = \sqrt{\frac{\varepsilon_0}{\mu_0}} N_2 \cos\theta_2 \overrightarrow{E_2} = \eta_2 \overrightarrow{E_2} \tag{11}$$

where N_2 is the complex refractive index of the substrate and θ_2 is the angle of refraction of light at interface II, and $\eta_2 = \sqrt{\frac{\varepsilon_0}{\mu_0}} N_2 \cos\theta_2$ is the admittance of the substrate.

By combining Equations (8), (9), (10) and (11), the relationship[3] between the electric field vectors of the incident and outgoing media on the Ni-plated silicon wafer can be obtained：

$$\overrightarrow{E_0}\begin{bmatrix} 1 \\ Y \end{bmatrix} = \begin{bmatrix} \overrightarrow{E_0} \\ \overrightarrow{H_0} \end{bmatrix} = \begin{bmatrix} cos\,\delta_1 & \frac{i}{\eta_1} sin\,\delta_1 \\ i\eta_1\, sin\,\delta_1 & cos\,\delta_1 \end{bmatrix} \begin{bmatrix} 1 \\ \eta_2 \end{bmatrix} \overrightarrow{E_2} = \begin{bmatrix} B \\ C \end{bmatrix} \overrightarrow{E_2} \tag{12}$$

where Y is the combined admittance of the silicon substrate with the Ni nanofilm, $\delta_1 = \frac{2\pi}{\lambda} N_1 h_1 \cos\theta_1$, and $\eta_1 = \sqrt{\frac{\varepsilon_0}{\mu_0}} N_1 \cos\theta_1$ is the admittance of the thin film nickel.

From (12), the characteristic matrix $\begin{bmatrix} B \\ C \end{bmatrix}$ of the Ni nanofilm system can be obtained as follows：

$$\begin{bmatrix} B \\ C \end{bmatrix} = \begin{bmatrix} cos\,\delta_1 & \frac{i}{\eta_1} sin\,\delta_1 \\ i\eta_1\, sin\,\delta_1 & cos\,\delta_1 \end{bmatrix} \begin{bmatrix} 1 \\ \eta_2 \end{bmatrix} \tag{13}$$

for a phase difference δ_1 generated by linearly polarized light passing through interfaces I and II, and admittance η_1 in an Ni medium. Because the Ni medium is the MO layer, it is known from Equation (4) that the refractive index N_1 can be divided into N_- and N_+, corresponding to the complex refractive indices of left and right circularly polarized light, respectively. The phase difference $\delta_1^{\mp}$ generated by the left and right circularly polarized light passing through interface I and interface II , and the corresponding admittance $\eta_1^{\mp}$ in the Ni medium, satisfy the following expression：

$$\begin{cases} \delta_1^{\pm} = \frac{2\pi}{\lambda} N_1 h_1\, cos\theta_1 = \frac{2\pi}{\lambda} N_{\pm} h_1\, cos\theta_1 = \frac{2\pi}{\lambda}\sqrt{\varepsilon_x}\left(1 \pm \frac{AM}{2}\right) h_1\, cos\,\theta_1 \\ \eta_1^{\pm} = \sqrt{\frac{\varepsilon_0}{\mu_0}} N_1\, cos\theta_1 = \sqrt{\frac{\varepsilon_0}{\mu_0}} N_{\pm}\, cos\theta_1 = \frac{2\pi}{\lambda}\sqrt{\varepsilon_x}\left(1 \pm \frac{AM}{2}\right) h_1\, cos\,\theta_1 \end{cases} \tag{14}$$

By combining Equations (11) and (13) with Equation (6), the relationship between the Kerr rotation angle θ_k and the magnetization M of the Ni nanofilm can be obtained under the excitation of an applied magnetic field $\overrightarrow{H_{applied}}$ as:

$$\begin{aligned} \theta_k = \mathrm{abs}(\mathrm{arc}&\left(\frac{i\eta_0\left((\eta_2\cos\delta_1^+ + i\eta_1^+\sin\delta_1^+)\left(\cos\delta_1^+ - i\frac{\eta_2}{\eta_1^+}\sin\delta_1^+\right) - \left(\cos\delta_1^+ + i\frac{\eta_2}{\eta_1^+}\sin\delta_1^+\right)(\eta_2\cos\delta_1^+ - i\eta_1^+\sin\delta_1^+)\right)}{\eta_0^2\left(\cos\delta_1^+ + i\frac{\eta_2}{\eta_1^+}\sin\delta_1^+\right)\left(\cos\delta_1^+ - i\frac{\eta_2}{\eta_1^+}\sin\delta_1^+\right) - \left(\cos\delta_1^+ + i\frac{\eta_2}{\eta_1^+}\sin\delta_1^+\right)(\eta_2\cos\delta_1^+ - i\eta_1^+\sin\delta_1^+)}\right) \\ - \mathrm{arc}&\left(\frac{i\eta_0\left((\eta_2\cos\delta_1^- + i\eta_1^-\sin\delta_1^-)\left(\cos\delta_1^- - i\frac{\eta_2}{\eta_1^-}\sin\delta_1^-\right) - \left(\cos\delta_1^- + i\frac{\eta_2}{\eta_1^-}\sin\delta_1^-\right)(\eta_2\cos\delta_1^- - i\eta_1^-\sin\delta_1^-)\right)}{\eta_0^2\left(\cos\delta_1^- + i\frac{\eta_2}{\eta_1^-}\sin\delta_1^-\right)\left(\cos\delta_1^- - i\frac{\eta_2}{\eta_1^-}\sin\delta_1^-\right) - \left(\cos\delta_1^- + i\frac{\eta_2}{\eta_1^-}\sin\delta_1^-\right)(\eta_2\cos\delta_1^- - i\eta_1^-\sin\delta_1^-)}\right)) \end{aligned} \tag{15}$$

Where $\delta_1^{\pm} = \frac{2\pi}{\lambda} N_1 h_1\, cos\theta_1 = \frac{2\pi}{\lambda}\sqrt{\varepsilon_x}\left(1 \pm \frac{AM}{2}\right) h_1 \cos\theta_1$, $\eta_1^{\pm} = \sqrt{\frac{\varepsilon_0}{\mu_0}} N_1\, cos\theta_1 = \frac{2\pi}{\lambda}\sqrt{\varepsilon_x}\left(1 \pm \frac{AM}{2}\right) h_1 \cos\theta_1$, arc means arctangent function. Thus, it can be seen from Equation (15) that there is a one-to-one relationship between the Kerr rotation angle θ_k and the magnetization M of the film.

B. COUPLING BETWEEN MAGNETIZATION AND TEMPERATURE

According to the mean field (MF) theory, the saturation magnetization[1,2,10,11] of an amorphous metal film with constituents can be expressed as：

$$M_s(T) = F_a u_B \sum_{i=1}^{n} x_i g_i J_i(\hat{T}) \tag{16}$$

where

$$F_a = \frac{0.95}{\left(\sum_i^n x_i V_i\right)} \tag{17}$$

$$J_i(\hat{T}) = J_i B_{J_i}(\xi) \tag{18}$$

F_a is the total number of metal atoms per unit volume; V_i is the atomic volume of each atom, which in the amorphous state is densely packed as hard spheres and occupies 95% of the space; x_i is the atomic coefficient of each atom, $\sum_{i=1}^{n} x_i = 1$; u_B is the Bohr magneton; g_i is the Lund factor of each atom, T is the film temperature; J_i is the total angular momentum quantum number of each metallic material, $B_{J_i}(\xi)$ is the Brillouin function, where

$$\xi = \frac{g_i u_B J_i H_i}{k_B T} \tag{19}$$

$$H_i = H_{applied} + \frac{2}{u_B g_i} \sum_{i=1}^{n} J_{ij} F_{ci} x_i J_i(\hat{T}) \tag{20}$$

ξ is the ratio of the Seeman energy of the magnetic moment to the random heat energy $k_B T$, k_B is the Boltzmann constant, $H_{applied}$ is the amplitude of the applied magnetic field, J_{ij} is the exchange integral between each atom, and F_{ci} is the coordination number of each atom.

The saturation magnetization can be viewed as the product of the total number of metal atoms per unit volume and the saturation magnetic moment of each metal atom. At the saturation magnetization of a ferromagnetic substance, the magnetic moments $\overrightarrow{m_s}$ of all metal atoms can be assumed to be roughly in the same direction as the applied magnetic field $\overrightarrow{H_{applied}}$. However, for superparamagnetic substances, there is a certain angle between the magnetic moment $\overrightarrow{m_s}$ of some metal atoms and the applied magnetic field $\overrightarrow{H_{applied}}$ due to thermal motion energy. Therefore, the total number of metal atoms per unit volume is modified such that Equation (16) can be applied to the relationship between saturation magnetization and temperature under superparamagnetism.

$$F_{modified} = \sum_{\tau=1}^{n=N} \overrightarrow{r_{m_s\tau}} \cdot \overrightarrow{r_H} = \mathrm{F}_a \cdot \Theta \tag{21}$$

where $\overrightarrow{r_{m_s\tau}}$ is the unit vector along the direction of the magnetic moment of the individual metal atoms, $\overrightarrow{r_H}$ is the unit vector along the direction of the applied magnetic field, Θ is a correction factor related to the applied magnetic field $\overrightarrow{H_{applied}}$, and the magnetic anisotropy constants K_u, K_d, and K_s [8] ,and K_u, K_d, K_s are the magnetic anisotropy constants between the magnetization vector and the uniaxial easy axis of the film, the film surface, and the surface, respectively.

When $n = 1$, i.e. $i = 1$, (16), (20) and (21) are combined to obtain the modified MF theory expression for the saturation magnetization of a single-component superparamagnetic transition metal film:

$$\begin{cases} M_{modified}(T) = F_{modified} x_1 g_1 J_1(\hat{T}) \\ J_1(\hat{T}) = (\frac{2J_1+1}{2}) coth(\frac{(2J_1+1)F_{c1}}{k_B T} J_{11} x_1 J_1(\hat{T})) - \frac{1}{2} coth(\frac{F_{c1}}{k_B T} J_{11} x_1 J_1(\hat{T})) \end{cases} \tag{22}$$

where $F_{modified}$ is the number of effective metal atoms per unit volume, x_1 is the Ni singlet atomic factor, g_1 is the Ni metal Lunde factor, J_1 is the total Ni metal angular momentum, F_{c1} is the Ni atom coordination number, and J_{11} is the exchange integral energy between Ni atoms.

For superparamagnetic nickel metal films, the magnetization in the direction of the external field can be described by the Langevin function[12]:

$$M(T) = M_{modified}(T)(coth(\frac{u_B m_s H_{applied}}{k_B T}) - \frac{k_B T}{u_B m_s H_{applied}}) \tag{23}$$

where $M_{modified}(T)$ is the saturation magnetization of the superparamagnetic Ni metal film, which can be determined from Equation (22), $H_{applied}$ is the amplitude of the applied magnetic field, and m_s is the saturation magnetic moment of the Ni atom. The relationship between the magnetization M of a superparamagnetic transition metal film and the film temperature T[9] can be obtained by combining Equations (22) and (23).

C. Theoretical model for temperature measurement

From Equation (23), it can be concluded that the magnetization strength M of a superparamagnetic film has a certain dependence on the film temperature T for a fixed applied magnetic field $H_{applied}$. The magnetization of the film M can then be expressed by Equation (23) in the form of a function $M(T)$ with respect to the film temperature T. From Equation (15) it can also be concluded that the Kerr rotation angle θ_k has a certain dependence on the film magnetization M. Then, the Kerr rotation angle θ_k can be expressed by Equation (15) as a function $\theta_k(M)$ with respect to the film magnetization M. Since the film magnetization M is dependent on the temperature T, the Kerr rotation angle θ_k can likewise be expressed as a function $\theta_k(T)$ with respect to the temperature T. Therefore, the theoretical model of temperature can be constructed as follows:

$$
\left\{
\begin{array}{l}
\theta_k=\mathrm{abs}(\mathrm{arc}\left(\dfrac{\mathrm{i}\eta_0\left((\eta_2\cos\delta_1^+ + \mathrm{i}\eta_1^+\sin\delta_1^+)\left(\cos\delta_1^+ - \mathrm{i}\frac{\eta_2}{\eta_1^+}\sin\delta_1^+\right) - \left(\cos\delta_1^+ + \mathrm{i}\frac{\eta_2}{\eta_1^+}\sin\delta_1^+\right)(\eta_2\cos\delta_1^+ - \mathrm{i}\eta_1^+\sin\delta_1^+)\right)}{\eta_0^2\left(\cos\delta_1^+ + \mathrm{i}\frac{\eta_2}{\eta_1^+}\sin\delta_1^+\right)\left(\cos\delta_1^+ - \mathrm{i}\frac{\eta_2}{\eta_1^+}\sin\delta_1^+\right) - \left(\cos\delta_1^+ + \mathrm{i}\frac{\eta_2}{\eta_1^+}\sin\delta_1^+\right)(\eta_2\cos\delta_1^+ - \mathrm{i}\eta_1^+\sin\delta_1^+)}\right) \\
\quad -\mathrm{arc}\left(\dfrac{\mathrm{i}\eta_0\left((\eta_2\cos\delta_1^- + \mathrm{i}\eta_1^-\sin\delta_1^-)\left(\cos\delta_1^- - \mathrm{i}\frac{\eta_2}{\eta_1^-}\sin\delta_1^-\right) - \left(\cos\delta_1^- + \mathrm{i}\frac{\eta_2}{\eta_1^-}\sin\delta_1^-\right)(\eta_2\cos\delta_1^- - \mathrm{i}\eta_1^-\sin\delta_1^-)\right)}{\eta_0^2\left(\cos\delta_1^- + \mathrm{i}\frac{\eta_2}{\eta_1^-}\sin\delta_1^-\right)\left(\cos\delta_1^- - \mathrm{i}\frac{\eta_2}{\eta_1^-}\sin\delta_1^-\right) - \left(\cos\delta_1^- + \mathrm{i}\frac{\eta_2}{\eta_1^-}\sin\delta_1^-\right)(\eta_2\cos\delta_1^- - \mathrm{i}\eta_1^-\sin\delta_1^-)}\right)) \\
\delta_1^\pm = \dfrac{2\pi}{\lambda}\sqrt{\varepsilon_x}\left(1 \pm \dfrac{AM(T)}{2}\right)h_1\cos\theta_1 \\
\eta_1^\pm = \dfrac{2\pi}{\lambda}\sqrt{\varepsilon_x}\left(1 \pm \dfrac{AM(T)}{2}\right)h_1\cos\theta_1 \\
M(T) = M_{modified}(T)(coth(\dfrac{u_B m_s H_{applied}}{k_B T}) - \dfrac{k_B T}{u_B m_s H_{applied}})
\end{array}
\right. \tag{24}
$$

According to Equation (24), θ_k has one-to-one correspondence with the temperature T, which can be back-calculated by measuring the value of θ_k.

REFERENCE

[1] Gangulee, A., and R. J. Kobliska. "Mean field analysis of the magnetic properties of amorphous transition - metal - rare - earth alloys." Journal of Applied Physics 49.9 (1978): 4896-4901.

[2] Heiman, Neil, et al. "Modified mean - field model for rare - earth - iron amorphous alloys." Journal of Applied Physics 47.6 (1976): 2634-2638.

[3] LI, Kai-hong, and Jin YANG. "Study of multi-layer antireflection coating by using character matrix of multi-layer dielectric film." Journal of Chengdu University of Information Technology (2006): S1.

[4] Pershan, P. S. "Magneto - optical effects." Journal of applied physics 38.3 (1967): 1482-1490.

[5] Hunt, Robert P. "Magneto - optic scattering from thin solid films." Journal of Applied Physics 38.4 (1967): 1652-1671.

[6] Chen, Liang - Yao, et al. "Kerr effect of two - medium layered systems." Journal of applied physics 67.12 (1990): 7547-7555.

[7] Fronk, M., et al. "Determination of the Voigt constant of phthalocyanines by magneto-optical Kerr-effect spectroscopy." Physical Review B 79.23 (2009): 235305.

[8] Shichang Z Z J D Z. Determination of K_1, K_u and y of YIG Magnetic Films for Easily Oriented (111) Plane by the FMR Method[J]. (1991).

[9] Callen, E., Y. J. Liu, and J. R. Cullen. "Initial magnetization, remanence, and coercivity of the random anisotropy amorphous ferromagnet." Physical Review B 16.1 (1977): 263.

[10] ZQ, Lu, et al. "Temperature Dependence of the Amorphous SmTbFeCo Magneto-Optical Films." Journal of the Magnetics Society of Japan 22.S_2_MORIS_97 (1998): S2_105-108.

[11] Hajjar, R., and Masud Mansuripur. "Mean-field analysis of ternary and quaternary rare earth-transition metal alloys for thermomagnetic recording." IEEE Transactions on Magnetics 25.5 (1989): 4021-4023.

[12] Zhong, Jing, et al. "A noninvasive, remote and precise method for temperature and concentration estimation using magnetic nanoparticles." Nanotechnology 23.7 (2012): 075703.